Optics Communications 444 (2019) 87–92

Contents lists available at ScienceDirect

Optics Communications

journal homepage: www.elsevier.com/locate/optcom

# On the performance of cognitive underlay RF/FSO communication systems with limited feedback

Eylem Erdogan

*Department of Electrical and Electronics Engineering, Istanbul Medeniyet University, Uskudar, Istanbul, Turkey*

ARTICLE INFO

*Keywords:*
Free space optical communication
Cognitive radio
Outage probability
Ergodic capacity
Exponentiated weibull fading

ABSTRACT

In this work, we consider an underlay cognitive radio (CR) RF/free space optical (FSO) network where the unlicensed secondary user (SU) wishes to communicate with a specific destination node with the aid of an optical path over a selected relay terminal without causing any interference to the primary user (PU). The proposed structure can be viable for metropolitans where an unlicensed user wishes to transfer its information to a specific destination node which is connected to the backbone network over an optical path. For the proposed structure, closed form and approximate outage probability and ergodic capacity expressions are derived for Nakagami-*m*/ Exponentiated Weibull fading channels. The results show that the transmission capacity of the SU depends on the weather conditions and the number of relays in the system.

## 1. Introduction

Wireless communication systems have been increasing at a rapid rate over the past years to meet the demand for high speed ubiquitous internet. To this end, two emerging technologies, 3rd Generation Partnership Project (3GPP) and Long term Evolution (LTE) have been developed recently [1,2]. Even though these new technologies can manage to meet the demand to a certain extent, the rapid increase in the mobile data traffic leads to the problem of spectrum scarcity.

One of the candidates for spectrum utilization is cognitive radio (CR). CR has emerged to alleviate the problem of spectrum utilization in wireless systems. In CR, the unlicensed user shares the same spectrum with the licensed user under specific constraints [3,4]. There are three spectrum sharing methods in CR; underlay, overlay and interweave [5,6]. In the underlay approach, the secondary user (SU) communicates with the same frequency band of the primary user (PU) without causing any interference. As a result, both spectrum efficiency and the throughput may increase. In the overlay approach, the SU helps the PU in the transmission by sharing its resources and hence it can communicate on a time-division multiplexing mode. In interweave model, the secondary network (SN) uses the frequency band of the primary network (PN) when the PN is not active. However, this approach is not practical as it may cause unwanted interference to the PN [7]. To leverage the advantages of CR and to enhance the coverage capacity of SUs, relay aided transmission, where the relays can amplify or decode and forward the received signal can be preferable. In the literature, relay aided transmission has been widely used in CR networks, e.g. [8,9].

Another candidate, optical wireless communication (OWC) can remedy the problem of spectrum scarcity by allowing license free spectrum with Gigabit throughput. OWC, specifically, free space optical (FSO) communication can provide easy deployment, power consumption and secure communication. Owing to its potentials, FSO systems are expected to be used in the last-mile access, campus connectivity and video monitoring in the next generation optical wireless communication systems. Even though FSO systems can bring numerous advantages, weather conditions can adversely affect the overall performance of the optical communication quality [10,11]. Several channel models have been introduced in the literature to model the atmospheric turbulence including Lognormal, $K$, Gamma–Gamma (GG) and Exponentiated Weibull (EW) fading. The classical distributions Lognormal, $K$ and GG can be used to model weak, strong or particular channel conditions [12,13]. Compared to its counterparts, EW fading can be used to model weak-to-strong turbulence induced fading for various aperture averaging conditions [14,15].

Most recently, employing FSO with RF transmission have attracted considerable interest as it can be a promising solution for the last mile connectivity problem. RF/FSO transmission can exploit the advantages of FSO systems while dealing with the spectrum scarcity problem. In the literature, RF/FSO transmission was investigated in [16–23] and the references therein. In [16,17], dual-hop hybrid RF/FSO system was investigated for decode-and-forward (DF) and amplify-and-forward (AF) RF/FSO networks respectively, where bit error rate, outage probability and ergodic capacity were derived for GG fading channels. Likewise, [18–23] elaborated the performance of RF/FSO systems over EW fading channels where important performance characteristics were derived.

CR-RF/FSO network can be considered as a spectrally efficient way of RF/FSO transmission as it can remedy the problem of spectrum

*E-mail address:* eylem.erdogan@medeniyet.edu.tr.

https://doi.org/10.1016/j.optcom.2019.03.074
Received 19 February 2019; Received in revised form 27 March 2019; Accepted 28 March 2019
Available online 1 April 2019

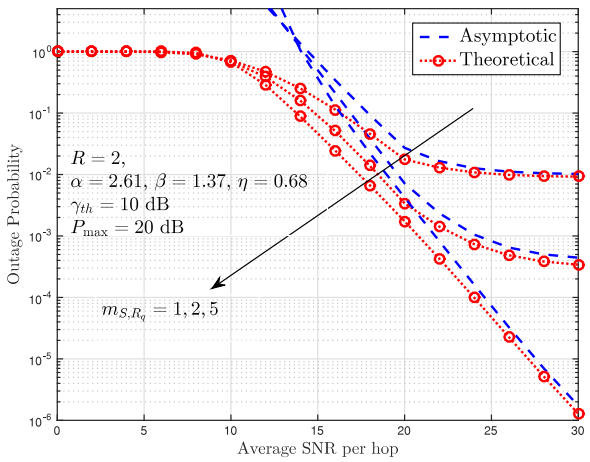


**Fig. 1.** Outage probability performance of the considered network for various Nakagami-$m$ severity parameters.

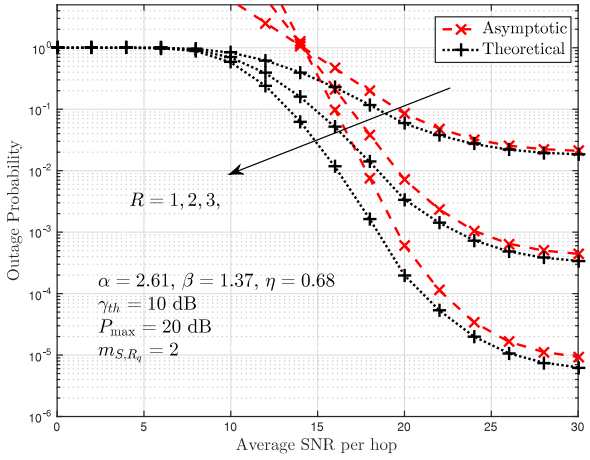


**Fig. 2.** Outage probability performance of the CR-RF/FSO network for different number of relays.

scarcity while reaping the advantages of RF/FSO networks. In CR-RF/FSO, SU transfers to its information to a specific node in the backbone network with the aid of an FSO link. Various studies have been devoted in the literature to investigate the CR-RF/FSO systems [16,24–27]. As Table 1 reveals, almost all the aforementioned works have considered on the outage probability analysis for GG fading at the FSO path. However, in this work, first time in the literature, we assume that the RF path experiences Nakagami-$m$ fading whereas the FSO link is distributed with the EW fading. In addition, we both derive closed form and approximate outage probability and ergodic capacity expressions respectively for single relay and multi-relay schemes with best relay selection. The results show that the transmission capacity of the SU depends both on the weather conditions and the number of relays in the system.

## 2. Signal and system model

Herein, we consider a dual-hop mixed CR-RF/FSO network in which the secondary source ($S$) communicates with the destination ($D$) via the $r$th DF relay node which is selected among $R$ relays with the aid of max–min selection . The selected relay can decode the received signal and then forward it to the $D$ through an FSO link. As the FSO transmission supports cost-effective, free license transmission with high data rates, the proposed scenario can be viable for the RF/FSO communication systems where the unlicensed SU wishes to transfer its information to a specific $D$ in the last-mile system. We assume that the proposed communication model works in the half-duplex fashion and the following subsections present the signal models for the RF and FSO transmissions.

### 2.1. RF transmission

In the RF part, secondary source transmits its information to the selected relay while adhering to the interference limitations of the PU. In the underlay approach, $S$ utilizes the spectrum of the PN as long as the interference of the PU–SU remains below the interference threshold $I_p$. The following subsection describes the power allocation scheme for the underlay approach.

#### 2.1.1. Mean-value power allocation

In the wide body of literature, it is assumed that the primary receiver has full knowledge of the interference channel information between the PN and the SN. However, in urban areas like metropolitans, fading varies fast and it becomes almost impossible for the primary receiver to have the full knowledge of the interference channel. To reduce the feedback burden, a practical power allocation scheme, mean-value (MV) power allocation has emerged considerable interest most recently [28,29]. In MV power allocation scheme (also known as limited feedback), the primary receiver obtains the mean value of the feedback gain and feds back to the secondary system. In this model, the secondary source power can be expressed as $P_S = \min\left\{\frac{I_p}{E[|h_{S,P}|^2]}, P_{\max}\right\}$, where $I_p$ is the maximum tolerable interference power at the primary receiver (PR), $P_{\max}$ is the maximum available power in the SN and $h_{S,P}$ is the channel coefficient of the interference link $S \to P$.

#### 2.1.2. Transmission protocol

At the beginning of the communication, $S$ transmits a pilot signal to the $D$ and the latter selects the best relay which maximizes the overall signal-to-noise ratio (SNR). The transmission between $S$ to $D$ is completed in two phases. In the first phase, $S$ transmits its information $x_s$ to the selected relay terminal. The received signal at the $r$ can be expressed as

$$y_r = \sqrt{\min\left\{\frac{I_p}{E[|h_{S,P}|^2]}, P_{\max}\right\}} h_{S,R_r} x_s + n_r, \tag{1}$$

where $h_{S,R_r}$ and $h_{S,P}$ are the channel informations between $S \to R$ and $S \to P$ which undergo independent but not identically distributed (i.n.i.d) Nakagami-$m$ fading channel with fading severity parameters $m_{S,R_r}$ and $m_{S,P}$ respectively, $n_r$ is the additive white Gaussian noise at the relay with $N_0$ noise power and $x_s$ is the information signal.

### 2.2. FSO transmission

In the second phase, the relay first filters out the DC components of the received signal with the aid of a band-pass filter. Thereafter, $R_r$ detects the source information, modulates it with the subcarrier intensity modulation and forwards to the $D$ after the modulated signal is properly biased. At the $D$, direct detection is employed by the photocurrent and the optical signal is converted to the electrical signal as

$$y_D = P_R h_{R_r,D} \zeta \tilde{x}_s + n_d, \tag{2}$$

where $\tilde{x}_s$ is the received source signal, $h_{R_r,D}$ is the optical channel gain which is modeled as EW fading, $n_d$ is the additive white Gaussian noise at the destination with $N_0$ noise power, $\zeta$ is the optical to electrical conversion ratio and $P_R$ is the relay power. By using (1) and (2) and with the aid of DF relaying, the e2e electrical SNR considering best relay selection, can be expressed as

$$\gamma_{e2e} = \max_{1 \le r \le R} (\min(\gamma_{S,R_r}, \gamma_{R_r,D})), \tag{3}$$

where $\gamma_{S,R_r} = \min\left\{\frac{I_p}{E[|h_{S,P}|^2]}, P_{\max}\right\} \frac{|h_{S,R_r}|^2}{N_0}$ and $\gamma_{R_r,D} = P_R \zeta^2 \frac{|h_{R_r,D}|^2}{N_0}$.

**Table 1**
Literature about CR-RF/FSO systems.

| Reference | System Model | RF Link | FSO Link | Interference Link | Performance Metrics |
|---|---|---|---|---|---|
| [24] | MIMO DF relaying | Rayleigh | GG | Rayleigh | Outage, Error Probability |
| [27] | AF relaying | Nakagami-$m$ | GG | Nakagami-$m$ | Outage Probability |
| [25] | MIMO DF relaying | Nakagami-$m$ | GG | Nakagami-$m$ | Outage Probability |
| [26] | MIMO AF relaying | Rayleigh | GG | Rayleigh | Outage Probability |

**Table 2**
List of notations and parameters.

| Parameter | Definition |
|---|---|
| $D$ | Receive aperture size |
| $L$ | Link distance |
| $\rho_0$ | Coherence radius |
| $\gamma_{th}$ | SNR threshold |
| $m_{S,R_r}$ | Fading severity parameter of the RF path |
| $m_{S,P}$ | Fading severity parameter of the interference channel |
| $\Gamma(\cdot)$ | Euler gamma function |
| $\alpha, \beta$ | Shape parameters of the EW fading |
| $\eta$ | Fading severity parameter of the EW fading |
| $P_{\max}$ | Maximum available power in the secondary network |
| $I_p$ | Maximum tolerable interference power |
| $\zeta$ | Optical to electrical conversion ratio |
| $G_{p,q}^{m,n}\left[\cdot \middle\vert \begin{matrix}\cdot\\ \cdot\end{matrix}\right]$ | Meijer-G function |
| $H_{p,q}^{m,n}\left[\cdot \middle\vert \begin{matrix}(\cdot,\cdot)\\ (\cdot,\cdot)\end{matrix}\right]$ | The H-function |

## 3. Fading statistics and outage probability analysis

### 3.1. Fading statistics of the RF channel

In the RF path, both $S \rightarrow R_r$ and $S \rightarrow P$ paths are modeled with Nakagami-$m$ distribution with fading severity parameters $m_{S,R_r}$ and $m_{S,P}$ respectively. Therefore, the CDF and the PDF of $\gamma_{S,R_r}$ can be expressed as [30]

$$F_{\gamma_{S,R_r}r}(\gamma) = 1 - \exp\left[-\frac{m_{S,R_r}\gamma}{\min\left\{\frac{\bar{I}_p}{E[|h_{S,P}|^2]}, \bar{P}_{\max}\right\}}\right] \times \sum_{z=0}^{m_{S,R_r}-1}\left(\frac{m_{S,R_r}\gamma}{\min\left\{\frac{\bar{I}_p}{E[|h_{S,P}|^2]}, \bar{P}_{\max}\right\}}\right)^z \frac{1}{z!}, \tag{4}$$

and

$$f_{\gamma_{S,R_r}}(\gamma) = \frac{\exp\left[-\frac{m_{S,R_r}\gamma}{\min\left\{\frac{\bar{I}_p}{E[|h_{S,P}|^2]}, \bar{P}_{\max}\right\}}\right]\left(\frac{m_{S,R_r}\gamma}{\min\left\{\frac{\bar{I}_p}{E[|h_{S,P}|^2]}, \bar{P}_{\max}\right\}}\right)^{m_{S,R_r}}}{\min\left\{\frac{\bar{I}_p}{E[|h_{S,P}|^2]}, \bar{P}_{\max}\right\}\Gamma(m_{S,R_r})}, \tag{5}$$

where $\bar{P}_{\max} = P_{\max}/N_0$ and $\bar{I}_p = I_p/N_0$.

### 3.2. Fading statistics of the FSO channel

As the FSO path follows EW fading, the PDF and the CDF of the channel can be expressed as [14,15]

$$f_{h_{S,R_r}}(I) = \frac{\alpha\beta}{\eta}\left(\frac{I}{\eta}\right)^{\beta-1}\exp\left[-\left(\frac{I}{\eta}\right)^{\beta}\right]\left(1-\exp\left[-\left(\frac{I}{\eta}\right)^{\beta}\right]\right)^{\alpha-1}, \tag{6}$$

and

$$F_{h_{S,R_r}}(I) = \left(1-\exp\left[-\left(\frac{I}{\eta}\right)^{\beta}\right]\right)^{\alpha}, \tag{7}$$

where $\alpha$, $\beta$ are the shape parameters and $\eta$ is the scale parameter. Notably, all notations and parameters are given in Table 2. With the aid of (7), the CDF of $\gamma_{R_r,D}$ can be obtained as

$$F_{\gamma_{R_r,D}}(\gamma) = \left(1-\exp\left[-\left(\frac{1}{\eta}\sqrt{\frac{\gamma}{\bar{\gamma}_{R_r,D}}}\right)^{\beta}\right]\right)^{\alpha}, \tag{8}$$

where $\bar{\gamma}_{R_r,D} = \frac{P_R}{N_0}\zeta^2$. By using Newton's generalized Binomial theorem, the above expression can be expressed as [31]

$$F_{\gamma_{R_r,D}}(\gamma) = \sum_{\rho=0}^{\infty}\binom{\alpha}{\rho}(-1)^{\rho}\exp\left[-\rho\left(\frac{\gamma}{\eta^2\bar{\gamma}_{R_r,D}}\right)^{\frac{\beta}{2}}\right]. \tag{9}$$

### 3.3. Closed form outage probability analysis

OP can be defined as the probability of SNR falling below a specified threshold $\gamma_{th}$. Mathematically, it can be expressed as

$$\begin{aligned} P_{\text{out}} &= \prod_{r}^{R}\left[1-\Pr[\gamma_{S,R_r} > \gamma_{th}]\Pr[\gamma_{R_r,D} > \gamma_{th}]\right] \\ &= \prod_{r}^{R}\left[1-(1-F_{\gamma_{S,R_r}}(\gamma_{th}))(1-F_{\gamma_{R_r,D}}(\gamma_{th}))\right]. \end{aligned} \tag{10}$$

By inserting (9) and (4) into (10), and after several manipulations, $P_{\text{out}}$ can be obtained as

$$\begin{aligned} P_{\text{out}} = \prod_{r}^{R}\Bigg[1-\Bigg\{1-\exp\left[-\frac{m_{S,R_r}\gamma}{\min\left\{\frac{\bar{I}_p}{E[|h_{S,P}|^2]}, \bar{P}_{\max}\right\}}\right] \\ \times \sum_{z=0}^{m_{S,R_r}-1}\left(\frac{m_{S,R_r}\gamma}{\min\left\{\frac{\bar{I}_p}{E[|h_{S,P}|^2]}, \bar{P}_{\max}\right\}}\right)^z\frac{1}{z!}\Bigg\} \\ \times\left\{1-\sum_{\rho=0}^{\infty}\binom{\alpha}{\rho}(-1)^{\rho}\exp\left[-\rho\left(\frac{\gamma}{\eta^2\bar{\gamma}_{R_r,D}}\right)^{\frac{\beta}{2}}\right]\right\}\Bigg]. \end{aligned} \tag{11}$$

If we apply Binomial expansion to the above expression [32, 1.111], $P_{\text{out}}$ can be expressed as

$$\begin{aligned} P_{\text{out}} = \sum_{r=0}^{R}\binom{R}{r}\Bigg[1-\Bigg\{\exp\left[-\frac{m_{S,R_r}\gamma}{\min\left\{\frac{\bar{I}_p}{E[|h_{S,P}|^2]}, \bar{P}_{\max}\right\}}\right] \\ \times \sum_{z=0}^{m_{S,R_r}-1}\left(\frac{m_{S,R_r}\gamma}{\min\left\{\frac{\bar{I}_p}{E[|h_{S,P}|^2]}, \bar{P}_{\max}\right\}}\right)^z\frac{1}{z!}\Bigg\}^r \\ \times\left\{1-\sum_{\rho=0}^{\infty}\binom{\alpha}{\rho}(-1)^{\rho}\exp\left[-\rho\left(\frac{\gamma}{\eta^2\bar{\gamma}_{R_r,D}}\right)^{\frac{\beta}{2}}\right]\right\}^{R-r}\Bigg]. \end{aligned} \tag{12}$$

With the aid of Multinomial expansion [32, 0.314], and after few manipulations, closed form OP can be obtained as

$$\begin{aligned} P_{\text{out}} = \sum_{r=0}^{R}\sum_{z=0}^{r(m_{S,R_r}-1)}\sum_{t=0}^{R-r}\sum_{\rho=0}^{\infty}\binom{R}{r}\binom{R-r}{t}\binom{\alpha t}{\rho}(-1)^{r+t+\rho}\gamma^z \\ \times \Xi_z(r)\exp\left[-\frac{rm_{S,R_r}\gamma_{th}}{\min\left\{\frac{\bar{I}_p}{E[|h_{S,P}|^2]}, \bar{P}_{\max}\right\}}\right]\exp\left[-\rho\left(\frac{\gamma_{th}}{\eta^2\bar{\gamma}_{R_r,D}}\right)^{\frac{\beta}{2}}\right], \end{aligned} \tag{13}$$

where $\Xi_r(t)$ stands for the Multinomial coefficients [32, 0.314].

### 3.4. Asymptotic outage probability analysis

At high SNR, OP can be expressed as

$$P_{\text{out}}^{\infty} = F_{\gamma_{S,R_r}}^{\infty}(\gamma_{th}) + F_{\gamma_{R_r,D}}^{\infty}(\gamma_{th}). \tag{14}$$

By substituting the high SNR approximation of $\exp(-x/a) \approx 1 - x/a$ into (4) and (8), asymptotic OP can be written as

$$P_{\text{out}} = \prod_{r=0}^{R}\left[\frac{1}{\Gamma(m_{S,R_r}+1)}\left(\frac{m_{S,R_r}\gamma_{th}}{\min\left\{\frac{\bar{I}_p}{E[|h_{S,P}|^2]}, \bar{P}_{\max}\right\}}\right)^{m_{S,R_r}} + \left(\frac{1}{\eta}\sqrt{\frac{\gamma_{th}}{\bar{\gamma}_{R_r,D}}}\right)^{\alpha\beta}\right]. \tag{15}$$

If we express $\bar{\gamma} = \kappa_A \min\left\{\frac{\bar{I}_p}{E[|h_{S,P}|^2]}, \bar{P}_{\max}\right\} = \kappa_B \bar{\gamma}_{R_r,D}$, the above expression can be expressed as

$$P_{out}^{\infty} = \mathcal{K}\left(\frac{\gamma_{th}}{\bar{\gamma}}\right)^{R\min(m_{S,R_r},\alpha\beta/2)} + \text{H.O.T.}, \tag{16}$$

where H.O.T. denotes the high order terms and $\mathcal{K}$ can be expressed as

$$\mathcal{K} = \begin{cases} \frac{1}{\Gamma(m_{S,R_r}+1)}\left(\kappa_A m_{S,R_r}\right)^{m_{S,R_r}}, & m_{S,R_r} < \alpha\beta/2 \\ \frac{1}{\Gamma(m_{S,R_r}+1)}\left(\kappa_A m_{S,R_r}\right)^{m_{S,R_r}} + \frac{\kappa_B^{1/2}}{\eta^{\alpha\beta}}, & m_{S,R_r} = \alpha\beta/2 \\ \frac{\kappa_B^{1/2}}{\eta^{\alpha\beta}}, & m_{S,R_r} > \alpha\beta/2. \end{cases} \tag{17}$$

From (17), the diversity gain of the overall network can be found as $\mathcal{G}_d = R\min(m_{S,R_r}, \alpha\beta/2)$. This equation shows that the overall diversity of the CR-RF/FSO system can be maximized in low fading/atmospheric turbulence conditions and when $R \gg 1$.

## 4. Ergodic capacity analysis

### 4.1. Closed form ergodic capacity analysis

Ergodic capacity ($C_{\text{erg}}$) can be defined as the maximum achievable capacity of the overall system. Mathematically speaking, it can be expressed as [30]

$$C_{\text{erg}} = \frac{1}{2}\mathbb{E}\left[\log_2(1+\gamma_{e2e})\right] = \frac{\log_2(e)}{2}\int_0^{\infty}\frac{1}{1+\gamma}\bar{F}_{\gamma_{e2e}}(\gamma)d\gamma, \tag{18}$$

where $\mathbb{E}[\cdot]$ denotes the expectation operation, 1/2 shows the total transmission time is 2 and $\bar{F}_{\gamma_{e2e}}(\gamma) = 1 - F_{\gamma_{e2e}}(\gamma)$. Note that, $\bar{F}_{\gamma_{e2e}}(\gamma)$ can be obtained by changing $\gamma_{th}$ with $\gamma$ in (13). By substituting $\bar{F}_{\gamma_{e2e}}(\gamma)$ into (18), $C_{\text{erg}}$ can be expressed as

$$C_{\text{erg}} = \frac{\log_2(e)}{2}\int_0^{\infty}\frac{1}{1+\gamma}\left\{1 - \sum_{r=0}^{R}\sum_{z=0}^{r(m_{S,R_r}-1)}\sum_{t=0}^{R-r}\sum_{\rho=0}^{\infty}\binom{R}{r}\binom{R-r}{t}\binom{\alpha t}{\rho}\Xi_z(r) \times (-1)^{r+t+\rho}\gamma^z \exp\left[-\frac{rm_{S,R_r}\gamma}{\min\left\{\frac{\bar{I}_p}{E[|h_{S,P}|^2]}, \bar{P}_{\max}\right\}}\right]\exp\left[-\rho\left(\frac{\gamma}{\eta^2\bar{\gamma}_{R_r,D}}\right)^{\frac{\beta}{2}}\right]\right\}d\gamma. \tag{19}$$

To the best of our knowledge the above expression cannot be evaluated in closed-form. However, we can obtain $C_{\text{erg}}$ for the following specific case.

#### 4.1.1. Ergodic capacity analysis for solo CR-RF/FSO transmission ($R = 1$)

In the proposed CR-RF/FSO model, if $R$ is selected as 1 in the transmission, the $F_{\gamma_{e2e}}(\gamma)$ can be expressed as

$$F_{\gamma_{e2e}}(\gamma) = 1 - \sum_{z=0}^{m_{S,R_r}-1}\binom{\alpha}{\rho}\left(\frac{m_{S,R_r}\gamma}{\min\left\{\frac{\bar{I}_p}{E[|h_{S,P}|^2]}, \bar{P}_{\max}\right\}}\right)^z\frac{1}{z!} \times \exp\left[-\frac{m_{S,R_r}\gamma}{\min\left\{\frac{\bar{I}_p}{E[|h_{S,P}|^2]}, \bar{P}_{\max}\right\}}\right]\left\{1 - \sum_{\rho=0}^{\infty}\binom{\alpha}{\rho}(-1)^{\rho} \times \exp\left[-\rho\left(\frac{\gamma}{\eta^2\bar{\gamma}_{R_r,D}}\right)^{\frac{\beta}{2}}\right]\right)^{\alpha}\right\}. \tag{20}$$

If we substitute (20) into (18), after changing the limits of the summation and with several manipulations, $C_{\text{erg}}^{R=1}$ can be expressed as

$$C_{\text{erg}}^{R=1} = \frac{\log_2(e)}{2}\sum_{z=0}^{m_{S,R_r}-1}\sum_{\rho=1}^{\infty}\binom{\alpha}{\rho}\left(\frac{m_{S,R_r}}{\min\left\{\frac{\bar{I}_p}{E[|h_{S,P}|^2]}, \bar{P}_{\max}\right\}}\right)^z\frac{(-1)^{\rho+1}}{z!} \times \int_0^{\infty}\frac{1}{1+\gamma}\gamma^z\exp\left[-\frac{m_{S,R_r}\gamma}{\min\left\{\frac{\bar{I}_p}{E[|h_{S,P}|^2]}, \bar{P}_{\max}\right\}}\right]\exp\left[-\rho\left(\frac{\gamma}{\eta^2\bar{\gamma}_{R_r,D}}\right)^{\frac{\beta}{2}}\right]d\gamma. \tag{21}$$

With the fact that $\frac{1}{\gamma+1} \approx \frac{1}{\gamma}$, with the aid of $\exp(-x) = G_{1,0}^{0,1}\left[x\middle|\begin{matrix}-\\0\end{matrix}\right]$ and after a few manipulations, the above expression can be written as

$$C_{\text{erg}}^{R=1} = \frac{\log_2(e)}{2}\sum_{z=0}^{m_{S,R_r}-1}\sum_{\rho=1}^{\infty}\binom{\alpha}{\rho}\left(\frac{m_{S,R_r}}{\min\left\{\frac{\bar{I}_p}{E[|h_{S,P}|^2]}, \bar{P}_{\max}\right\}}\right)^z\frac{(-1)^{\rho+1}}{z!} \times \int_0^{\infty}\gamma^{z-1}G_{1,0}^{0,1}\left[\frac{m_{S,R_r}\gamma}{\min\left\{\frac{\bar{I}_p}{E[|h_{S,P}|^2]}, \bar{P}_{\max}\right\}}\middle|\begin{matrix}-\\0\end{matrix}\right]\exp\left[-\rho\left(\frac{\gamma}{\eta^2\bar{\gamma}_{R_r,D}}\right)^{\frac{\beta}{2}}\right]d\gamma. \tag{22}$$

Please note that $G_{p,q}^{m,n}\left[\cdot\middle|\begin{matrix}\cdot\\\cdot\end{matrix}\right]$ denotes the Meijer-G function [33, 07.34.02.0001.01]. The above expression is still tedious if not possible to obtain a closed form. However, if we assume that $\mathcal{A} = \rho\left(\frac{1}{\eta^2\bar{\gamma}_{R_r,D}}\right)^{\frac{\beta}{2}}$, and after changing the variables in the above expression as $x = \mathcal{A}\gamma^{\beta/2}$, $C_{\text{erg}}^{R=1}$ can be expressed as

$$C_{\text{erg}}^{R=1} = \frac{\log_2(e)}{2}\sum_{z=0}^{m_{S,R_r}-1}\sum_{\rho=1}^{\infty}\binom{\alpha}{\rho}\left(\frac{m_{S,R_r}}{\min\left\{\frac{\bar{I}_p}{E[|h_{S,P}|^2]}, \bar{P}_{\max}\right\}}\right)^z\frac{(-1)^{\rho+1}}{z!}\left(\frac{2}{\beta\mathcal{A}}\right) \times \int_0^{\infty}\left(\frac{x}{\mathcal{A}}\right)^{\frac{2}{\beta}z-1}G_{1,0}^{0,1}\left[\frac{m_{S,R_r}x^{\frac{2}{\beta}}}{\mathcal{A}^{\frac{2}{\beta}}\min\left\{\frac{\bar{I}_p}{E[|h_{S,P}|^2]}, \bar{P}_{\max}\right\}}\middle|\begin{matrix}-\\0\end{matrix}\right]G_{1,0}^{0,1}\left[x\middle|\begin{matrix}-\\0\end{matrix}\right]dx. \tag{23}$$

A closed form solution for the above expression can be found by using the integral form of two Meijer-G functions as [33, 07.34.21.0012.01]

$$C_{\text{erg}}^{R=1} = \frac{\log_2(e)}{2}\sum_{z=0}^{m_{S,R_r}-1}\sum_{\rho=1}^{\infty}\binom{\alpha}{\rho} \times \left(\frac{m_{S,R_r}}{\min\left\{\frac{\bar{I}_p}{E[|h_{S,P}|^2]}, \bar{P}_{\max}\right\}}\right)^z\frac{(-1)^{\rho+1}}{z!}\left(\frac{2}{\beta}\right)\left(\frac{1}{\mathcal{A}}\right)^{\frac{2}{\beta}z} \times H_{1,1}^{1,1}\left[\frac{m_{S,R_r}}{\mathcal{A}^{\frac{2}{\beta}}\min\left\{\frac{\bar{I}_p}{E[|h_{S,P}|^2]}, \bar{P}_{\max}\right\}}\middle|\begin{matrix}\left(1-\frac{2}{\beta}z, \frac{2}{\beta}\right)\\(0,1)\end{matrix}\right], \tag{24}$$

where $H_{p,q}^{m,n}\left[\cdot\middle|\begin{matrix}(\cdot,\cdot)\\(\cdot,\cdot)\end{matrix}\right]$ denotes the Fox H-function [34].

### 4.2. Approximate ergodic capacity analysis

Ergodic capacity can be tightly upper bounded by the following approximation

$$C_{\text{erg}} = \frac{1}{2}\mathbb{E}\left[\log_2(1+\gamma_{e2e})\right] \approx C_{\text{erg}}^{\text{up}} = \frac{1}{2}\log_2(1+\mathbb{E}\left[\gamma_{e2e}\right]). \tag{25}$$

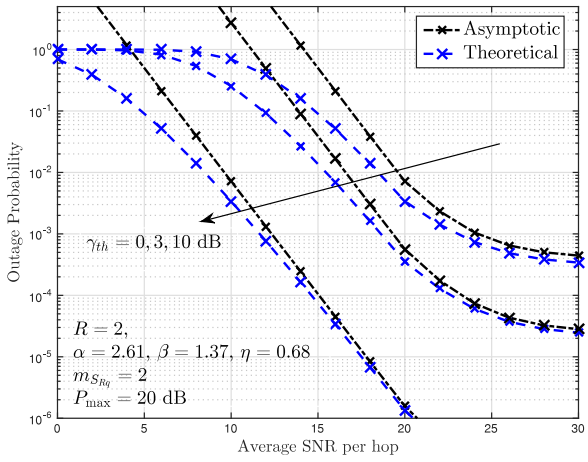


**Fig. 3.** Outage probability performance of the proposed network for different threshold values.

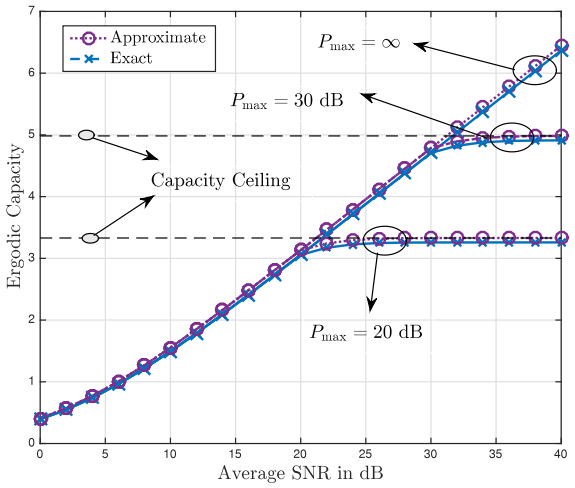


**Fig. 4.** Ergodic capacity performance of the considered scheme for different $P_{\max}$ values when $(\alpha, \beta, \eta) = (3.52, 2.15, 0.76)$.

With the aid of (3), $C_{\text{erg}}^{\text{up}}$ can be expressed as

$$C_{\text{erg}}^{\text{up}} = \frac{1}{2}\log_2\left(1 + \max_{1\le r\le R} \min(\mathbb{E}\left[\gamma_{S,R_r}\right], \mathbb{E}\left[\gamma_{R_r,D}\right])\right). \tag{26}$$

$\mathbb{E}\left[\gamma_{S,R_r}\right]$ can be obtained as

$$\begin{aligned}\mathbb{E}\left[\gamma_{S,R_r}\right] &= \int_0^\infty (1 - F_{\gamma_{S,R_r}}(\gamma))d\gamma \\ &= \int_0^\infty \exp\left[-\frac{m_{S,R_r}\gamma}{\min\left\{\frac{\bar{I}_p}{E[|h_{S,P}|^2]}, \bar{P}_{\max}\right\}}\right] \\ &\quad \times \sum_{z=0}^{m_{S,R_r}-1}\left(\frac{m_{S,R_r}\gamma}{\min\left\{\frac{\bar{I}_p}{E[|h_{S,P}|^2]}, \bar{P}_{\max}\right\}}\right)^z \frac{1}{z!}d\gamma \\ &= \sum_{z=0}^{m_{S,R_r}-1}\frac{1}{z!}\left(\frac{m_{S,R_r}}{\min\left\{\frac{\bar{I}_p}{E[|h_{S,P}|^2]}, \bar{P}_{\max}\right\}}\right)^{-1}\Gamma[z+1],\end{aligned} \tag{27}$$

whereas $\mathbb{E}\left[\gamma_{R_r,D}\right]$ can be obtained as

$$\begin{aligned}\mathbb{E}\left[\gamma_{R_r,D}\right] &= \int_0^\infty (1 - F_{\gamma_{R_r,D}}(\gamma))d\gamma \\ &= \int_0^\infty \sum_{t=1}^{\infty}\binom{\alpha}{t}(-1)^{t+1}\exp\left[-t\left(\frac{\gamma}{\eta^2\bar{\gamma}_{R_r,D}}\right)^{\frac{\beta}{2}}\right]d\gamma \\ &= \sum_{t=1}^{\infty}\binom{\alpha}{t}(-1)^{t+1}t^{-2/\beta}\left(\frac{1}{\eta^2\bar{\gamma}_{R_r,D}}\right)^{-1}\Gamma[1+2/\beta].\end{aligned} \tag{28}$$

By substituting (28) and (27) into (24), $C_{\text{erg}}^{\text{up}}$ can be obtained.

## 5. Numerical results

In this section, theoretical results are verified with the asymptotic curves to demonstrate the performance of the proposed scheme. In the simulations, various link distances and fading models are used to show the outage probability and ergodic capacity performance of the CR-RF/FSO system. Outage curves are obtained for $\gamma_{th} = 10$ dB, $D = 60$ mm, $(\alpha, \beta, \eta) = (2.61, 1.37, 0.68)$ for moderate turbulence induced fading whereas ergodic capacity curves are plotted for $(\alpha, \beta, \eta) = (3.52, 2.15, 0.76)$, $(2.69, 0.43, 0.178)$, for $D = 25{,}100$ mm respectively to demonstrate moderate and strong turbulences at the FSO path. In addition, for notational brevity, without loss of generality, we assume $I_p = P_r$ and $m_{S,P} = 1$ in all figures.

Fig. 1 shows the OP performance of the CR-RF/FSO scheme for various Nakagami-$m$ fading severity parameters. As can be seen from the figure, as the number of fading severity parameters increase, the performance improves and the diversity gain enhances up to 3.75. For the three curves, the overall diversity gain can be calculated with the aid of $\mathcal{G}_d = R\min(m_{S,R_r}, \alpha\beta/2)$ as 2, 3.75 and 3.75 respectively and these analytical calculations can be verified with the slopes of the curves. In addition, when $P_{\max} = 20$, the OP performance saturates and approaches to zero diversity and error floor occurs. It is also important to note that the asymptotic results are in good agreement with the theoretical derivations.

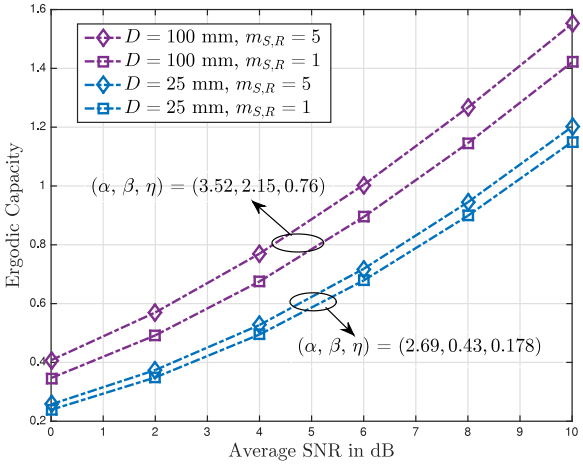


**Fig. 5.** Ergodic capacity performance of the CR-RF/FSO scheme for various channel conditions . (For interpretation of the references to color in this figure legend, the reader is referred to the web version of this article.)

Fig. 2 depicts the OP performance of the considered scheme for different number of relays. Observed from the figure that, as the number of relays increase, both the system performance and the diversity gain enhances. However, as the power reaches to its peak value, $P_{\max} = 20$, the performance saturates and goes to zero diversity. Notably, this figure verifies that the increase in the relay number solely enhances the overall diversity gain and the system performance.

Different from Figs. 1 and 2, Fig. 3 shows the impact of the threshold $\gamma_{th}$ for acceptable communication quality. As can be seen, as $\gamma_{th}$ increases, the performance degrades. It is important to note that, if $\gamma_{th}$ is selected as $\gamma_{th} > 0$ dB, $P_{\max}$ adversely affects the diversity gain of the overall system. Thereby, selecting a lower $\gamma_{th}$ may lead to a better performance.

Fig. 4 shows the ergodic capacity performance of the CR-RF/FSO system for moderate turbulence induced fading $(\alpha, \beta, \eta) = (3.52, 2.15, 0.76)$ and $m_{S,R_r} = 5$. It is important to note that the curves in this figure are plotted with the aid of (21) and (26). As shown in the figure, the capacity ceiling occurs at $P_{\max} = 20$ dB and $P_{\max} = 30$ dB where the capacity of the system saturates. Moreover, as observed from the figure, the approximate findings are in good agreement with the and exact results.

Fig. 5 illustrates the performance of the CR-RF/FSO system for different receive aperture sizes, $D = 25, 100$ mm with moderate and strong turbulence induced fading $(\alpha, \beta, \eta) = (3.52, 2.15, 0.76), (2.69, 0.43, 0.178)$ respectively, when $m_{S,R_r} = 1$ and $m_{S,R_r} = 5$. As shown in the figure, in the presence of strong turbulence induced fading with small aperture size, the blue curves and the purple ones differ approximately 0.3 bits/channel use at 10 dB. More precisely, as the strong fading at the FSO path offers more channel fluctuations, the throughput of the overall system increases and the degradation due to small receiver aperture diminishes. Owing to this, the capacity difference between two curves is at minimum.

## 6. Conclusions

As FSO communication supports cost-effective, free license transmission with high data rates, we propose a novel spectrally efficient CR-RF/FSO scheme in which the secondary source wishes to transmit its information to a specific destination in the backbone network without causing any interference to the primary system. Such a system can be viable in metropolitans where an unlicensed user tries to communicate with another user in the backbone network through RF and FSO paths respectively. Another practical implementation of the proposed scheme can be considered as the university campuses which are overwhelmed with intense network traffic. To quantify the performance of the proposed scheme, we derived closed form outage probability and ergodic capacity expressions. The theoretical findings which can help a system designer to get an idea about the overall performance, show that the performance of the secondary user can be enhanced in the presence of light turbulence and fading affects when $R \gg 1$.

## Acknowledgment

This work was supported by the Research Fund of Istanbul Medeniyet University, Turkey. Project Number: F-GAP-2017-1056.

## References

[1] Ericsson, Mobile data surpasses voice, stockholm, sweden, 2010, (Online), Available: http://www.ericsson.com/thecompany/press/releases/2010/03/1396928.
[2] E. Dahlman, S. Parkvall, S. J, B. P, 3G Evolution: HSPA and LTE for Mobile Broadband, Academic Press, New York, 2010.
[3] S. Haykin, et al., Cognitive radio: brain-empowered wireless communications, IEEE J. Sel. Areas Commun. 23 (2) (2005) 201–220.
[4] J. Mitola, G.Q. Maguire, Cognitive radio: making software radios more personal, IEEE Personal Commun. 6 (4) (1999) 13–18.
[5] W. Liang, S.X. Ng, L. Hanzo, Cooperative overlay spectrum access in cognitive radio networks, IEEE Commun. Surv. Tutor. 19 (3) (2017) 1924–1944.
[6] E. Biglieri, A.J. Goldsmith, L.J. Greenstein, H.V. Poor, N.B. Mandayam, Principles of Cognitive Radio, Cambridge University Press, 2013.
[7] S.K. Sharma, T.E. Bogale, S. Chatzinotas, B. Ottersten, L.B. Le, X. Wang, Cognitive radio techniques under practical imperfections: A survey, IEEE Commun. Surv. Tutor. (2015).
[8] Q. Zhang, J. Jia, J. Zhang, Cooperative relay to improve diversity in cognitive radio networks, IEEE Commun. Mag. 47 (2) (2009) 111–117.
[9] P.L. Yeoh, M. Elkashlan, K.J. Kim, T.Q. Duong, G.K. Karagiannidis, Transmit antenna selection in cognitive MIMO relaying with multiple primary transceivers, IEEE Trans. Veh. Technol. 65 (1) (2016) 483–489.
[10] G.K. Varotsos, H.E. Nistazakis, W. Gappmair, H.G. Sandalidis, G.S. Tombras, Df relayed subcarrier FSO links over malaga turbulence channels with phase noise and non-zero boresight pointing errors, Appl. Sci. 8 (5) (2018) 2076–3417.
[11] F. Bai, Y. Su, T. Sato, Performance analysis of heterodyne-detected OCDMA systems using PolSK modulation over a free-space optical turbulence channel, Electronics 4 (4) (2015) 785–798.
[12] B. Epple, Simplified channel model for simulation of free-space optical communications, J. Opt. Commun. Netw. 2 (5) (2010) 293–304.
[13] X. Yi, Z. Liu, P. Yue, Formula for the average bit error rate of free-space optical systems with dual-branch equal-gain combining over gamma-gamma turbulence channels, Opt. Lett. 38 (2) (2013) 208–210.
[14] R. Barrios, F. Dios, Exponentiated weibull distribution family under aperture averaging for Gaussian beam waves, Opt. Express 20 (12) (2012) 13055–13064.
[15] R. Barrios, F. Dios, Exponentiated weibull model for the irradiance probability density function of a %laser beam propagating through atmospheric turbulence, Opt. Laser Technol. 45 (2) (2013) 13–20.
[16] E. Zedini, I.S. Ansari, M. Alouini, Performance analysis of mixed Nakagami-$m$ and Gamma-Gamma dual-hop FSO transmission systems, IEEE Photonics J. (ISSN: 1943-0655) 7 (1) (2015) 1–20.
[17] S. Anees, M.R. Bhatnagar, Performance of an amplify-and-forward dual-hop asymmetric RF/FSO communication system, IEEE/OSA J. Opt. Commun. Networking (ISSN: 1943-0620) 7 (2) (2015) 124–135.
[18] J. Zhao, Shang-Hong, Wei-Hu, Y. Liu, X. Li, Performance of mixed RF/FSO systems in exponentiated weibull distributed channels, Opt. Commun. 405 (2017) 244–252.
[19] Y. Zhang, X. Wang, S.H. Zhao, J. Zhao, B.-y. Deng, On the performance of 2× 2 DF relay mixed RF/FSO airborne system over Exponentiated Weibull fading channel, Opt. Commun. 425 (2018) 190–195.
[20] Y. Wang, P. Wang, X. Liu, T. Cao, On the performance of dual-hop mixed RF/FSO wireless communication system in urban area over aggregated Exponentiated Weibull fading channels with pointing errors, Opt. Commun. 410 (2018) 609–616.
[21] Z. Jing, Z. Shang-hong, Z. Wei-hu, C. Ke-fan, Performance analysis for mixed FSO/RF Nakagami-m and Exponentiated Weibull dual-hop airborne systems, Opt. Commun. 392 (2017) 294–299.
[22] X. Yi, C. Shen, P. Yue, Y. Wang, Q. Ao, Performance of decode-and-forward mixed RF/FSO system over $\kappa$- $\mu$ shadowed and Exponentiated Weibull fading, Opt. Commun. 439 (2019) 103–111.
[23] E. Erdogan, Joint user and relay selection for relay-aided RF/FSO systems over Exponentiated Weibull fading channels, Opt. Commun. 436 (2019) 209–215.
[24] N. Varshney, A.K. Jagannatham, P.K. Varshney, Cognitive mimo-rf/fso cooperative relay communication with mobile nodes and imperfect channel state information, arXiv preprint arXiv:1805.05381 (2018).
[25] N. Varshney, A.K. Jagannatham, Cognitive decode-and-forward mimo-rf/fso cooperative relay networks, IEEE Commun. Lett. 21 (4) (2017) 893–896.
[26] F.S. Al-Qahtani, A.H.A. El-Malek, I.S. Ansari, R.M. Radaydeh, S.A. Zummo, Outage analysis of mixed underlay cognitive RF MIMO and FSO relaying with interference reduction, IEEE Photonics J. 9 (2) (2017) 1–22.
[27] H. Arezumand, H. Zamiri-Jafarian, E. Soleimani-Nasab, Outage and diversity analysis of underlay cognitive mixed RF-FSO cooperative systems, J. Opt. Commun. Netw. 9 (10) (2017) 909–920.
[28] E. Erdogan, A.S. Afana, H.U. Sokun, S.S. Ikki, L. Durak-Ata, H. Yanikomeroglu, Signal space cognitive cooperation, IEEE Trans. Veh. Technol. (2018).
[29] A. Afana, I.A. Mahady, S. Ikki, Quadrature spatial modulation in MIMO cognitive radio systems with imperfect channel estimation and limited feedback, IEEE Trans. Commun. 65 (3) (2017) 981–991.
[30] M.K. Simon, M.S. Alouini, Digital Communication Over Fading Channels, vol. 95, John Wiley & Sons, 2005.
[31] E. Erdogan, Joint user and relay selection for relay-aided RF/FSO systems over Exponentiated Weibull fading channels, Opt. Commun. (2018).
[32] I.S. Gradshteyn, I.M. Ryzhik, Table of Integrals, Series, and Products, Academic press, 2014.
[33] From wolframresearch—the mathematical functions site, http://functions.wolfram.com.
[34] A.M. Mathai, R.K. Saxena, H.J. Haubold, The H-Function: Theory and Applications, Springer Science & Business Media, 2009.